

# On the polarization characteristics of Mössbauer coherent scattering by perfect magnetic-ordered crystals

V. A. Belyakov and E. V. Smirnov

All-Union Research Institute of Physico-technical and Radio Measurements

(Submitted June 26, 1974)

Zh. Eksp. Teor. Fiz. 68, 608-622 (February 1975)

Resonant coherent scattering of Mössbauer  $\gamma$  radiation by perfect magnetically ordered crystals is considered theoretically. It is shown that the characteristics of coherent Mössbauer-radiation scattering, and in particular its polarization properties, significantly depend on the details of the crystal magnetic structure, differ qualitatively from the case of Mössbauer-radiation scattering in paramagnetic crystals, and can be expressed in terms of the properties of the proper solutions of the Maxwell equations for the Mössbauer  $\gamma$  quanta in the crystal. For crystals of arbitrary thickness, expressions are found for the intensities and polarizations of the  $\gamma$  beams coherently scattered and transmitted through the crystal. The analysis is carried out in the two-wave approximation of the dynamic diffraction theory. Numerical calculations are performed for scattering by a ferromagnetic iron crystal. The most characteristic manifestations of Mössbauer-radiation scattering by magnetically ordered crystals are noted, viz., the "three-hump" shape of the reflection curve, six beat periods in the Pendellosung, and the possibility of obtaining polarization of scattered radiation under controlled experimental conditions.

## 1. INTRODUCTION

Theoretical and experimental investigations of coherent scattering of Mössbauer radiation from crystals have revealed many features of this radiation, of interest both to solid-state physics and to nuclear physics (see, e.g., [1-10], where additional references can be found). Considerable attention is attracted, in particular, by the investigation of the Mössbauer coherent scattering by magnetically-ordered crystals and by crystals in which the Mössbauer nuclei are located in sites with zero electric-field gradient. In such crystals, for example, the anomalously large transparency of the medium to Mössbauer radiation can become most clearly pronounced (the effect of suppression of inelastic nuclear channels) [1,10]. Another interesting property of Mössbauer scattering by magnetically ordered crystals (and more generally by crystals in which hyperfine splitting of the Mössbauer spectrum exists) is the dependence of the polarization characteristics of coherent scattering on the structure of magnetic (hyperfine) fields in the crystal. However, the question of the polarization properties has been considered in detail only for Mössbauer scattering by thin crystals [3,11]. In the case of crystals of arbitrary thickness, the polarization characteristics were investigated for the simplest situations [9,12].

In this paper we analyze the polarization properties of Mössbauer coherent scattering in magnetically ordered perfect crystals of arbitrary thickness. One stage of this analysis is the determination of the eigen-solutions of Maxwell's equations for Mössbauer radiation under conditions when the Bragg conditions are satisfied and the investigation of the polarization properties of the eigensolutions. It turns out that the polarizations of the eigensolutions are directly connected with the magnetic structure of the crystal, are not orthogonal to one another in a typical situation, and vary with changing  $\gamma$ -quantum energy as well as with the deviation of the scattering angle from the exact Bragg condition. The aforementioned polarization properties, in conjunction with different damping decrements of the eigensolutions, lead to a qualitative difference between the Mössbauer scattering by magnetically ordered crystals and x-ray or Mössbauer scattering by nonmag-

netic crystals. In particular, the scattered radiation can have a polarization that is almost complete and depends on the magnetic structure of the crystal although the initial radiation is not polarized. The polarization of the scattered radiation and that transmitted through the crystal turns out to be dependent on the energy of the  $\gamma$  quanta and on the thickness of the crystal.

The nonorthogonality of the polarizations of the natural waves leads to unique interference phenomena which do not appear in the scattering of other types of radiation by crystals. Thus, in the pendulum (Pendellosung) effect it is possible for six periods of the beats of the scattering intensity to appear with varying thickness of the crystal (or energy of the  $\gamma$  quantum), unlike the two periods in the case of x rays. In this paper, in addition to a general analysis of the polarization properties of the Mössbauer scattering and their connection with the magnetic structure of the crystal, we consider in detail concrete situations that are of interest from the experimental point of view and lead to simplification of the general expressions. Numerical calculations are performed for some of the cases.

## 2. SYSTEM OF DYNAMIC EQUATIONS

We consider the scattering of Mössbauer radiation by a magnetically ordered crystal containing Mössbauer nuclei, at quantum incidence angles satisfying the Bragg condition. To find the electromagnetic field in the crystal, it is necessary to solve Maxwell's equations which, as is well known [9,10], reduce under the conditions in question to the following system of equations:

$$\begin{aligned}(k_1^2/\kappa^2 - 1)E_1 &= \hat{F}_{11}E_1 + \hat{F}_{12}E_2, \\ (k_2^2/\kappa^2 - 1)E_2 &= \hat{F}_{21}E_1 + \hat{F}_{22}E_2,\end{aligned}\quad (1)$$

where  $\kappa$  is the wave vector of the  $\gamma$  quantum in vacuum, while  $k_1$ ,  $k_2$ ,  $E_1$ , and  $E_2$  are the wave vectors and amplitudes of the primary and diffracted waves in the crystal. The operator  $\hat{F}_{ip}$ , the form of which is given below, describes the scattering of a wave with wave vector  $k_p$  into a wave with wave vector  $k_i$  by the unit cell of the crystal. The wave vectors in (1) are connected by the Bragg condition

$$k_1 - k_2 = \tau, \quad (2)$$

where  $\tau/2\pi$  is the crystal reciprocal-lattice vector. Using the connection between  $\mathbf{k}_1$  and  $\mathbf{k}_2$ , which follows from the boundary conditions for a crystal in the form of a plane-parallel plate, we can represent the system (1) in the form

$$[\varepsilon\hat{I} - 1/2\hat{b}(\hat{F} - \hat{\delta})]\tilde{\mathbf{E}} = (\varepsilon\hat{I} - \hat{\Phi})\tilde{\mathbf{E}} = 0, \quad (3)$$

where  $\hat{I}$  is a unit matrix of fourth order;

$$\tilde{\mathbf{E}} = \begin{pmatrix} \mathbf{E}_1 \\ \mathbf{E}_2 \end{pmatrix} = A \begin{pmatrix} \mathbf{n} \\ B\mathbf{n}' \end{pmatrix}$$

(here  $A$  and  $B = |\mathbf{E}_2|/|\mathbf{E}_1|$  are scalar quantities, while  $\mathbf{n}$  and  $\mathbf{n}'$  are the polarization vectors of the primary and diffracted waves);  $\hat{F}$  is the matrix of the coefficients of the right-hand side of system (1). The four-row matrices  $\hat{b}$  and  $\hat{\delta}$  are specified by the relations  $b_{ik} = \delta_{ik}$  if  $i \leq 2$ ,  $b_{ik} = b\delta_{ik}$  if  $i > 2$ ,  $(\delta)_{ik} = 0$  if  $i > 2$ , and  $(\delta)_{ik} = \delta\delta_{ik}$  if  $i > 2$ , where  $b = \cos \mathbf{k}_1 \mathbf{s} / \cos \mathbf{k}_2 \mathbf{s}$ ,  $\mathbf{s}$  is the unit vector normal to the plane of the crystal and directed to the interior of the crystal; the quantity  $\delta = \tau(\tau + 2\kappa)/\kappa^2$  characterizes the deviation of the angle of incidence of the radiation on the crystal from the exact Bragg condition;

$$\varepsilon = (k_1^2/\kappa^2 - 1); \quad k_2^2/\kappa^2 - 1 = \delta + \varepsilon/b.$$

The condition under which the system (3) has a solution, namely

$$\det \{ \varepsilon\hat{I} - 1/2\hat{b}(\hat{F} - \hat{\delta}) \} = 0 \quad (4)$$

determines  $\varepsilon$ , i.e., the values of the wave vectors  $\mathbf{k}_1$  and  $\mathbf{k}_2$ , while the solution of the system (3) yields the corresponding amplitudes  $\mathbf{E}_1$  and  $\mathbf{E}_2$  as functions of the incidence angle (or  $\delta$ ) of the primary wave on the crystal. Thus, from the number of roots of Eq. (4) we obtain four eigensolutions of the system (3), and the field in the crystal is represented by a superposition of the eigensolutions:

$$\tilde{\mathbf{E}}(\mathbf{r}, t) = \sum_{p=1}^4 C_p (\mathbf{n}_p \exp\{i\mathbf{k}_p \mathbf{r}\} + B_p \mathbf{n}'_p \exp\{i\mathbf{k}'_p \mathbf{r}\}) e^{-i\omega t}, \quad (5)$$

in which the index  $p$  labels quantities pertaining to the  $p$ -th eigensolution. The coefficients  $C_p$  in (5) are determined from the boundary conditions on the amplitude of the primary and diffracted waves.

### 3. EIGENSOLUTIONS OF DYNAMIC SYSTEM

To obtain a general expression for the eigensolutions of the system (3), it is convenient to resolve the vectors of the natural polarizations  $\mathbf{n}_p$  and  $\mathbf{n}'_p$  along of the polarization unit vectors in the form

$$\begin{aligned} \mathbf{n}_p &= a_{1p}\chi_1(1) + a_{2p}\chi_2(1), \\ \mathbf{n}'_p &= (a_{3p}\chi_1(2) + a_{4p}\chi_2(2))/B_p, \end{aligned} \quad (6)$$

where  $\chi_1(1)$  and  $\chi_1(2)$  are the polarization unit vectors for directions 1 and 2, respectively. In this case  $B_p$  turns out to be identically equal to  $(|a_{3p}|^2 + |a_{4p}|^2)^{1/2}$ , and the quantities  $a_{ip}$  are expressed in terms of the elements of the matrix  $F$  (written in turn in terms of the unit vectors  $\chi_1(1)$  and  $\chi_1(2)$ ), the eigenvalues  $\varepsilon_p$  of Eq. (4), and the parameters  $\delta$  and  $b$  by the relations

$$a_{ip} = AD(\varepsilon_p)_{ki}, \quad d(\varepsilon_p) = \varepsilon_p \hat{I} - 1/2\hat{b}(\hat{F} - \hat{\delta}), \quad (7)$$

where  $D_{ki}$  is the cofactor of the element  $d_{ki}$  of the matrix  $d(\varepsilon_p)$  defined in the second relation of (7), while  $A$  is a normalization coefficient. Thus, the coefficients of the expansion of the field amplitudes in terms of the

polarization unit vectors are expressed in the eigensolution in terms of the cofactors of the elements of any row of the matrix  $d(\varepsilon_p)$ . For the sake of argument we assume that they are expressed in terms of the cofactors in the first row. Representing the vectors of the natural polarizations in the universally accepted form

$$\begin{aligned} \mathbf{n}_p &= (\cos \alpha_p \chi_1(1) + e^{i\beta_p} \sin \alpha_p \chi_2(1)) e^{i\eta_p}, \\ \mathbf{n}'_p &= (\cos \alpha'_p \chi_1(2) + e^{i\beta'_p} \sin \alpha'_p \chi_2(2)) e^{i\eta'_p}, \end{aligned} \quad (8)$$

we obtain for the parameters  $\alpha$ ,  $\beta$ , and  $\eta$  the expressions

$$\begin{aligned} \cos \alpha_p &= |a_{2p}|, \quad e^{i\beta_p} = \frac{a_{2p}}{|a_{2p}|}, \quad \text{tg } \alpha_p e^{i\beta_p} = \frac{a_{1p}}{a_{2p}}, \\ \cos \alpha'_p &= |a_{4p}|, \quad e^{i\beta'_p} = \frac{a_{4p}}{|a_{4p}|}, \quad \text{tg } \alpha'_p e^{i\beta'_p} = \frac{a_{3p}}{a_{4p}}. \end{aligned} \quad (9)$$

The foregoing formulas, which connect directly the polarization of the eigenwaves and the quantities  $B_p$  with the magnetic structure of the crystal, contain also the dependence on the parameter (the angle of incidence) and determine all the singularities and the polarization characteristics of coherent Mössbauer scattering by a magnetically-ordered crystal.

Since the analysis of the presented eigensolutions calls in general for numerical methods, because one of its stages is the determination of the roots of the fourth-degree equation (4), we note here some general properties of the eigensolutions.

Certain properties of the eigensolutions follow directly from the form of the matrix  $\hat{F} = \hat{F}(\mathbf{R}) + F(\mathbf{N})$ , the Rayleigh component  $F(\mathbf{R})$  of which coincides with the corresponding matrix for the diffraction of x rays<sup>[13]</sup>, and the nuclear component  $\hat{F}(\mathbf{N})$  can be represented in the form

$$F_{lm}^{(N)sp} = \frac{4\pi}{V\kappa^2} \sum_q f_{\text{coh}}^{(q)}(\mathbf{k}_m \chi_p(m), \mathbf{k}_l \chi_s(l)) \exp\{i(\mathbf{k}_m - \mathbf{k}_l) \mathbf{r}_q\}, \quad (10)$$

where  $f_{\text{coh}}(\mathbf{k} \cdot \mathbf{e}; \mathbf{k}' \cdot \mathbf{e}')$  is the amplitude of the coherent scattering of  $\gamma$  quantum with wave vector  $\mathbf{k}$  and polarization vector  $\mathbf{e}$  into a quantum with wave vector  $\mathbf{k}'$  and polarization vector  $\mathbf{e}'$  by a Mössbauer nucleus,  $V$  is the volume of the unit cell of the crystal, the vector  $\mathbf{r}$  specifies the position of the Mössbauer nucleus in the cell, the summation is over all the Mössbauer nuclei within the unit cell, and the subscript  $q$  labels quantities pertaining to the  $q$ -th Mössbauer nucleus.

Since the expression for the coherent nuclear amplitude contains energy denominators that contain the imaginary quantity  $i\Gamma/2$ <sup>[3,14]</sup>, the matrix of Eq. (3) (see (10)) is in the general case not Hermitian. Consequently, the polarizations of the eigensolutions are generally speaking not orthogonal to one another, i.e.,  $\mathbf{n}_p \cdot \mathbf{n}'_p \neq 0$  and  $\mathbf{n}'_p \cdot \mathbf{n}'_p \neq 0$ .

Since the matrix of Eq. (3) contains the parameter  $\delta$  which characterizes the angle of incidence of the radiation on the crystal in the region of the diffraction reflection, the polarization of the eigensolution turns out to be in the general case to depend not only on the magnetic structure but also on  $\delta$ . Outside the region of the diffraction reflection ( $\delta \rightarrow \pm\infty$ ) for the two eigensolutions we have  $|\mathbf{E}_2|/|\mathbf{E}_1| \rightarrow 0$ , and the eigenpolarizations of the wave  $\mathbf{E}_1$  tend to the eigenpolarizations for the direct passage of Mössbauer radiation in the direction of  $\mathbf{k}_1$ .<sup>[15]</sup> The two other eigensolutions correspond to direct passage in the  $\mathbf{k}_2$  direction.

#### 4. SOLUTION OF THE BOUNDARY-VALUE PROBLEM

If the wave incident on the crystal has a polarization vector  $\mathbf{e} = \cos \alpha \chi_2(1) + e^{i\beta} \sin \alpha \chi_1(1)$ , then in the Laue case ( $b > 0$ ), using the boundary conditions

$$\sum_p C_p B_p \mathbf{n}_p' = 0, \quad \sum_p C_p \mathbf{n}_p = \mathbf{e},$$

we obtain from (5) for the intensity of the radiation passing through the crystal in the primary and secondary directions

$$\begin{aligned} I_T(\mathbf{e}) &= \sum_{p=1}^4 |C_p(\mathbf{e})|^2 |\gamma_p|^2 \\ &+ 2\text{Re} \sum_{p>k} C_p(\mathbf{e}) C_k^*(\mathbf{e}) \gamma_p \gamma_k^* (\mathbf{n}_p \mathbf{n}_k'), \\ I_R(\mathbf{e}) &= \sum_{p=1}^4 |C_p(\mathbf{e})|^2 |\gamma_p|^2 B_p^2 \\ &+ 2\text{Re} \sum_{p>k} C_p(\mathbf{e}) C_k^*(\mathbf{e}) \gamma_p \gamma_k^* B_p B_k (\mathbf{n}_p' \mathbf{n}_k''). \end{aligned} \quad (11)$$

where

$$C_p(\mathbf{e}) = \Delta_{Lp}(\mathbf{e}) / \Delta_L,$$

$\Delta_L$  is the determinant of the matrix  $a_{ik}$  (see (7)),  $\Delta_{Lp}(\mathbf{e})$  is the determinant obtained from  $\Delta_L$  by putting in its  $p$ -th column

$$\begin{aligned} a_{1p} &= e^{i\beta} \sin \alpha, \quad a_{2p} = \cos \alpha, \quad a_{3p} = a_{4p} = 0, \\ \gamma_p &= \exp\{i e_p \mu L / 2 \cos \mu s\}, \end{aligned}$$

and  $L$  is the thickness of the crystal.

The polarization vectors of the radiation passing through the crystal are determined by the relations

$$\mathbf{n}_r(\mathbf{e}) = \frac{\sum_p C_p(\mathbf{e}) \gamma_p \mathbf{n}_p}{\left| \sum_p C_p(\mathbf{e}) \gamma_p \mathbf{n}_p \right|}, \quad \mathbf{n}_r(\mathbf{e}) = \frac{\sum_p C_p(\mathbf{e}) B_p \gamma_p \mathbf{n}_p'}{\left| \sum_p C_p(\mathbf{e}) B_p \gamma_p \mathbf{n}_p' \right|}. \quad (12)$$

As follows from (11) and (12), the intensities and the polarizations of the radiation in the primary and secondary directions produce beats as functions of the crystal thickness (the Pendellosung effect). Unlike x rays, for which there exist two periods of beats in the Mössbauer diffraction, owing to the non-orthogonality of the eigenpolarizations (of the vectors  $\mathbf{n}_p$ ) it is possible in the general case to realize six periods of beats in terms of the different values of the quantities  $\epsilon_p - \epsilon_{p'}$  with  $p \neq p'$ , which determine the periods of the beats. For a fixed crystal thickness, the beats manifest themselves in a change of the energy of the  $\gamma$  quanta, in connection with the energy dependence of the amplitudes, and hence of the differences  $\epsilon_p - \epsilon_{p'}$ . As follows from (11), the eigenwaves corresponding to the zeroth roots of (4) propagate through the crystal without being damped, i.e., for the corresponding waves there is the effect of suppression of the inelastic channels<sup>[1,10]</sup>.

In the case of an unpolarized primary beam we obtain from (11) for the intensities of the radiation passing through the crystal

$$\begin{aligned} I_T &= \frac{1}{2|\Delta_L|^2} \left\{ \sum_{i=1,2} |\Delta_{Lp}^i|^2 |\gamma_p|^2 \right. \\ &\left. + 2\text{Re} \sum_{p>k} \Delta_{Lp}^i \Delta_{Lk}^{i*} \gamma_p \gamma_k^* (\mathbf{n}_p \mathbf{n}_k') \right\}, \\ I_R &= \frac{1}{2|\Delta_L|^2} \left\{ \sum_{i=1,2} |\Delta_{Lp}^i|^2 B_p^2 |\gamma_p|^2 + 2\text{Re} \sum_{p>k} \Delta_{Lp}^i \Delta_{Lk}^{i*} B_p B_k \gamma_p \gamma_k^* (\mathbf{n}_p' \mathbf{n}_k'') \right\} \end{aligned} \quad (13)$$

where  $\Delta_{Lp}^1 \equiv \Delta_{Lp}$  at  $\alpha = 0$  and  $\Delta_{Lp}^2 \equiv \Delta_{Lp}$  at  $\alpha = \pi/2$  and  $\beta = 0$ .

The beams passing through the crystal are partly polarized and are described by the following polarization density matrices:

$$\begin{aligned} \rho_T &= \frac{1}{I_T} \sum_{i=1,2} I_T(\chi_i) \rho(\mathbf{n}_T(\chi_i)), \\ \rho_R &= \frac{1}{I_R} \sum_{i=1,2} I_R(\chi_i) \rho(\mathbf{n}_R(\chi_i)), \end{aligned} \quad (14)$$

where  $\rho(\mathbf{e})$  is the polarization matrix of the photon density with polarization vector  $\mathbf{e}$ .

In experiment, as a rule, one observes quantities that are integrated over the angle (in the Bragg-reflection region) and over the energy. The integration of expressions (12) with respect to  $\delta$  causes the results of the polarization measurements to be described, even in the case of a fully polarized primary beam, by a polarization matrix corresponding to a partly-polarized beam:

$$\begin{aligned} \bar{\rho}_T(\mathbf{e}) &= \frac{\int I_T(\mathbf{e}, \delta) \rho(\mathbf{n}_T(\mathbf{e}, \delta)) d\delta}{\int I_T(\mathbf{e}, \delta) d\delta}, \\ \bar{\rho}_R(\mathbf{e}) &= \frac{\int I_R(\mathbf{e}, \delta) \rho(\mathbf{n}_R(\mathbf{e}, \delta)) d\delta}{\int I_R(\mathbf{e}, \delta) d\delta}. \end{aligned} \quad (15)$$

An analogous procedure is used for averaging over the energy with allowance for the line shape of the primary beam, the scatterer, and if necessary the detector (for a resonant detector).

In the Bragg case ( $b < 0$ ), using the boundary conditions

$$\sum_p C_p \mathbf{n}_p = \mathbf{e}, \quad \sum_p C_p B_p \mathbf{n}_p' \exp(ik_z^p s L) = 0,$$

we obtain for the coefficient  $C_p$  in the expansion (5)

$$C_p(\mathbf{e}) = \frac{\Delta_{Bp}(\mathbf{e})}{\Delta_B}, \quad \Delta_B = \det \begin{pmatrix} a_{11} & a_{12} & a_{13} & a_{14} \\ a_{21} & a_{22} & a_{23} & a_{24} \\ \gamma_1 a_{31} & \gamma_2 a_{32} & \gamma_3 a_{33} & \gamma_4 a_{34} \\ \gamma_1 a_{41} & \gamma_2 a_{42} & \gamma_3 a_{43} & \gamma_4 a_{44} \end{pmatrix}. \quad (16)$$

The determinant  $\Delta_{Bp}(\mathbf{e})$  is obtained from  $\Delta_B$  in the same manner as  $\Delta_{Lp}(\mathbf{e})$  is obtained from  $\Delta_L$  (see formula (11)); the remaining notation in (16) is the same as before.

The intensity and polarization  $J_T(\mathbf{c})$  and  $\mathbf{n}_T(\mathbf{c})$  of the radiation transmitted through the crystal are determined, just as before, by the first relations in formulas (11)–(15), but with coefficients  $C_p$  defined by formula (16). The determinants  $\Delta_{Bp}^i$ , which now enter in (13), are connected with  $\Delta_B$  by the same connection as between  $\Delta_{Lp}^i$  and  $\Delta_L$ .

The corresponding values for the radiation reflected from the crystal are described by the expressions

$$I_R(\mathbf{e}) = \sum_{p=1}^4 |C_p(\mathbf{e})|^2 B_p^2 + 2\text{Re} \sum_{p>k} C_p(\mathbf{e}) C_k^*(\mathbf{e}) B_p B_k (\mathbf{n}_p' \mathbf{n}_k''), \quad (17)$$

$$\mathbf{n}_R(\mathbf{e}) = \sum_p C_p(\mathbf{e}) B_p \mathbf{n}_p' / \left| \sum_p C_p(\mathbf{e}) B_p \mathbf{n}_p' \right|, \quad (18)$$

$$I_R = \frac{1}{2|\Delta_B|^2} \left\{ \sum_{i=1,2} |\Delta_{Bp}^i|^2 B_p^2 + 2\text{Re} \sum_{p>k} \Delta_{Bp}^i \Delta_{Bk}^{i*} B_p B_k (\mathbf{n}_p' \mathbf{n}_k'') \right\}. \quad (19)$$

Just as in the Laue case, the intensities and the polarizations of the beams transmitted through the crystal and reflected from it experience beats with changing thickness of the crystal and with changing  $\gamma$ -ray energy.

We present the explicit form of the eigensolutions of the system (3) for a biquadratic secular equation. The case of a biquadratic equation is realized for the conditions of physical interest in a diffraction experiment, for example, if a magnetically preferred (say antiferromagnetic) axis exists in a cubic crystal, and the vectors  $\mathbf{k}_1$  and  $\mathbf{k}_2$  make equal angles with this axis.

To analyze this case, it is advantageous to use as the polarization unit vectors in (3) the unit vectors of the eigenpolarizations for direct passage in directions 1 and 2. In terms of these unit vectors, the matrix  $\hat{F}$  becomes simpler, since its elements, which describe scattering through zero angle, take the form

$$\hat{F}_{ii} = \begin{pmatrix} F_{i1}^{11} & 0 \\ 0 & F_{i2}^{22} \end{pmatrix},$$

and the relation  $F_{11}^{11} - F_{11}^{22} = F_{22}^{11} - F_{22}^{22}$  is satisfied for the diagonal elements. For the symmetrical Bragg case ( $b = -1$ ), the condition under which the secular equation (4) becomes biquadratic is

$$F_{12}^{12} F_{21}^{21} - F_{21}^{12} F_{12}^{21} = 0. \quad (20)$$

When condition (20) is satisfied, the eigenvalues and eigensolutions of (4) (see formula (7)), in terms of unit vectors that coincide with the eigenpolarization vectors for the direct transmission, are determined by the formulas

$$\begin{aligned} \bar{\epsilon} &= \epsilon - \frac{1}{4}(F_{11}^{11} + F_{11}^{22} - F_{22}^{11} - F_{22}^{22}) - \frac{\delta}{2} \\ &= \frac{1}{\sqrt{2}} \left\{ \frac{\delta^2}{2} - \delta(g_{11} + g_{22}) + (g_{11}^2 + g_{22}^2 - \Delta_+) \right. \\ &\quad \left. \pm \left\{ (g_{11} - g_{22})^2 \left[ \delta^2 - 2\delta(g_{11} + g_{22}) \left( 1 + \frac{F_{21}^{22} F_{12}^{22} - F_{12}^{11} F_{21}^{11}}{g_{11}^2 - g_{22}^2} \right) \right] \right. \right. \\ &\quad \left. \left. + g_{11}^2 + g_{22}^2 - \Delta_+ - 4 \det \hat{F} \right\}^{1/2} \right\}^{1/2}; \quad (21) \end{aligned}$$

$$\begin{aligned} a_{1p} &= (\bar{\epsilon}_p - a)^{-1} [F_{12}^{11} F_{21}^{11} (\bar{\epsilon}_p^2 - g^2) + F_{12}^{12} F_{21}^{21} (g + \bar{\epsilon}_p) + \Delta_1 \Delta_2], \\ a_{2p} &= F_{12}^{22} F_{21}^{21} (a + \bar{\epsilon}_p) + F_{12}^{21} F_{21}^{11} (g + \bar{\epsilon}_p), \quad a_{3p} = F_{21}^{11} (\bar{\epsilon}_p^2 - g^2) + F_{12}^{22} \Delta_2, \\ a_{4p} &= -[F_{12}^{21} \Delta_2 + F_{21}^{21} (g - \bar{\epsilon}_p) (a + \bar{\epsilon}_p)]. \quad B_p = \frac{[|a_{3p}|^2 + |a_{4p}|^2]^{1/2}}{[|a_{2p}|^2 + |a_{1p}|^2]^{1/2}}, \quad (22) \end{aligned}$$

where

$$\begin{aligned} a &= 1/2(F_{11}^{11} + F_{22}^{11} - \delta), \quad g = 1/2(F_{11}^{22} + F_{22}^{22} - \delta), \quad g_{11} = 1/2(F_{11}^{11} - F_{22}^{11}), \\ g_{22} &= 1/2(F_{11}^{22} - F_{22}^{22}), \\ \Delta_1 &= \det \hat{F}_{12}, \quad \Delta_2 = \det \hat{F}_{21}, \quad \Delta_+ = F_{12}^{12} F_{21}^{21} + F_{12}^{11} F_{21}^{11} + F_{12}^{22} F_{21}^{22} + F_{21}^{12} F_{12}^{21}. \end{aligned}$$

Formulas (21) and (22) determine completely the eigensolutions of the system of dynamic equations. Under the same conditions, the secular equation for the Laue case reduces to a biquadratic one at

$$F_{21}^{22} F_{12}^{22} - F_{12}^{11} F_{21}^{11} = 0.$$

The formulas presented in this section describe the reflection and transmission of Mössbauer radiation and its polarization characteristics for crystals of arbitrary thickness with any type of magnetic ordering. Of considerable practical interest are the limiting cases of thin and thick crystals, for which the analysis of the results becomes much simpler.

## 5. DIFFRACTION REFLECTION FROM THICK CRYSTALS

In the case of thin crystals  $\text{Im } \mathbf{k}_1^p \mathbf{s}L \ll 1$  ( $p = 1, 2, 3, 4$ ), formulas (17)–(19) go over into the well-known expressions of the kinematic theory<sup>[3]</sup>. For thick crystals,  $\text{Im } \mathbf{k}_1^p \mathbf{s}L \gg 1$ , only two of the four eigenwaves are excited in the crystal in the Bragg case, namely those having the maximum damping. The contribution of the two other eigenwaves to the solution (5) turns out to be exponentially small. Assuming that the maximum damping is possessed by eigensolutions 1 and 2, we obtain from (16) for the coefficients  $C_p$ , which do not contain small quantities,

$$C_1(e) = \frac{e^{i\beta} \sin \alpha a_{22} - \cos \alpha a_{12}}{a_{11} a_{22} - a_{21} a_{12}}, \quad C_2(e) = \frac{\cos \alpha a_{11} - e^{i\beta} \sin \alpha a_{21}}{a_{11} a_{22} - a_{21} a_{12}}, \quad (23)$$

which coincides with the expansion coefficients of the amplitude of the incident waves in the eigenpolarization unit vectors  $\mathbf{n}_1$  and  $\mathbf{n}_2$ . In this case the reflection curves of the waves whose polarizations coincide with the eigenpolarizations are described by the angular dependence of the quantities  $B_1$  and  $B_2$ . It must be borne in mind here that, generally speaking, the eigenpolarizations vary along the reflection curve. Since the eigenpolarizations  $\mathbf{n}'_1$  and  $\mathbf{n}'_2$  are not orthogonal in the general case, it follows that the reflection curve for unpolarized radiation is not simply the arithmetic mean of the curves for  $\mathbf{n}'_1$  and  $\mathbf{n}'_2$ , but contains also an interference increment. The reflection coefficients then take the form

$$\bar{R} = 1/2(1 - |\mathbf{n}_1 \mathbf{n}_2^*|^2)^{-1} [B_1^2 + B_2^2 - 2 \text{Re } B_1 B_2 (\mathbf{n}'_1 \mathbf{n}'_2^*) (\mathbf{n}_1 \mathbf{n}_2^*)]. \quad (24)$$

The polarization density matrix of the scattered radiation is described by the expression

$$\bar{\rho} = A \{ B_1^2 \rho(\mathbf{n}'_1) + B_2^2 \rho(\mathbf{n}'_2) - B_1 B_2 [(\mathbf{n}'_1 \mathbf{n}'_2) \rho(12) + (\mathbf{n}'_2 \mathbf{n}'_1) \rho(21)] \}, \quad (25)$$

where the matrices  $\rho(\mathbf{ik})$  are specified by the relations  $\rho(\mathbf{ik})_{pq} = n_i^* n_j^* \rho_{ij}$ , and  $A$  is a normalization factor. The matrix (25) corresponds to a scattered-radiation degree of polarization

$$P = \frac{2[(f^-)^2 + |D|^2]^{1/2}}{B_1^2 + B_2^2 - 2B_1 B_2 \text{Re}[(\mathbf{n}'_1 \mathbf{n}'_2) (\mathbf{n}'_1 \mathbf{n}'_2^*)]}. \quad (26)$$

The vector of the polarization that is partly represented in the scattered radiation is determined, in terms of the unit vectors  $\chi_1(2)$  and  $\chi_2(2)$  (see (6)), by the parameters  $\alpha$  and  $\beta$ , which satisfy the relation

$$\text{tg } \alpha e^{i\beta} = D \{ [(f^-)^2 + |D|^2]^{1/2} - f^- \}, \quad (27)$$

where

$$\begin{aligned} f^- &= 1/2 \{ B_1^2 (|\mathbf{n}'_1|^2 - |\mathbf{n}'_2|^2) + B_2^2 (|\mathbf{n}'_2|^2 - |\mathbf{n}'_1|^2) \\ &\quad - 2B_1 B_2 \text{Re}[(\mathbf{n}'_1 \mathbf{n}'_2) (\mathbf{n}'_1 \mathbf{n}'_2^*) - \mathbf{n}'_1 \mathbf{n}'_2 \mathbf{n}'_2 \mathbf{n}'_1^*] \}, \\ D &= B_1^2 \mathbf{n}'_1 \mathbf{n}'_2 + B_2^2 \mathbf{n}'_2 \mathbf{n}'_1 - B_1 B_2 [(\mathbf{n}'_1 \mathbf{n}'_2) \mathbf{n}'_1 \mathbf{n}'_2 + (\mathbf{n}'_2 \mathbf{n}'_1) \mathbf{n}'_2 \mathbf{n}'_1^*], \end{aligned}$$

and  $n_{pm}$  is the projection of the vector  $n_p$  on the  $m$ -th polarization unit vector. From (25) and (26), just as in the preceding section, we can obtain the characteristics integrated over the incidence angles and over the  $\gamma$ -ray energy.

Using expressions (23)–(27), we can analyze the general character of the dependence of the intensity of the reflected radiation and its polarization on small changes of the incidence angle near the Bragg condition. For the sake of argument, we shall assume below that a symmetrical Bragg case is realized. It is convenient to consider first the case of the Hermitian matrix

$\hat{F} - \hat{\delta}$ , which corresponds to neglect of absorption. In this case it follows from the properties of the solutions of the system (3) that  $B_i \equiv 1$  if the root  $\epsilon_i$  of the secular equation (4) is complex. This means that in the entire range of angles  $\Delta\theta$  (or of the corresponding values of the parameter  $\delta$ ), where all four roots of the secular equation (4) are complex, the reflection coefficient of a wave with any polarization becomes equal to unity. In the range of angles where two roots are real and two are complex, the reflection coefficient reaches unity only for a preferred proper polarization that is determined by the solution that attenuates in the interior of the crystal. In the region of four real roots, the reflection coefficient for a wave with any polarization is smaller than unity. Large angles of deviation from the Bragg condition correspond to four real roots of (4) and to a reflection coefficient  $R$  that tends to zero. Therefore a typical reflection curve of unpolarized radiation takes the form shown in Fig. 1.

The parameter ranges  $\delta_1 < \delta < \delta_2$  and  $\delta_5 < \delta < \delta_6$  correspond to two real and two complex roots of the secular equation. In these regions, the reflection coefficient is  $R \approx 1/2$ . The reflected radiation is fully polarized, and its polarization vector coincides with the polarization vector determined by the second relation in (8) for the eigensolution that attenuates in the interior of the crystal. In the region  $\delta_3 < \delta < \delta_4$  we have  $R = 1$ , and the reflected radiation is not polarized. Figure 1 shows a situation in which the region of total reflection of any polarization is separated from the region of selective reflection of the polarization. Depending on the concrete form of the matrix  $\hat{F}$ , the positions of the regions of total and selective reflection may change. In particular, one or both regions of the selective reflection can be directly adjacent to the total-reflection region.

When absorption is taken into account, the general "three-hump" character of the reflection curve is preserved. Everywhere, however, with the possible exception of individual points, the reflection coefficient turns out to be smaller than in the absence of absorption (this qualitative behavior is shown by the dashed curve of Fig. 1).

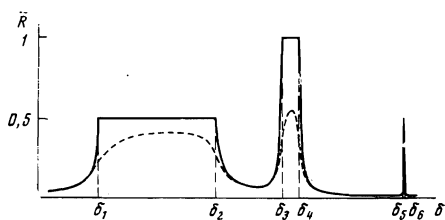


FIG. 1. Typical picture of reflection of unpolarized radiation from a magnetically ordered crystal (solid curve—without allowance for absorption, dashed—with allowance for absorption).

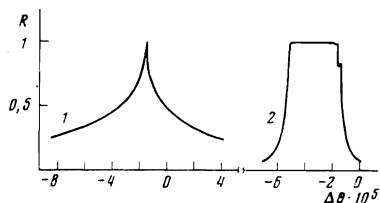


FIG. 2. Reflection curves for the eigenpolarizations (1—eigenwave strongly interacts with the nuclei, 2—eigenwave weakly interacts with the nuclei). Bragg reflection (110),  $\eta = 80\%$ ,  $\gamma$ -quantum energy  $E = E_{3/2-1/2}$ ,  $\Phi = 0$ .

The formulas of the present section and of the two preceding sections solves in general the diffraction problem not only for magnetic hyperfine splitting of the Mössbauer line in the crystal, but actually also for quadrupole and combined hyperfine splittings (actually, nowhere did we use the explicit form of the operator  $\hat{F}$ ).

## 6. RESULTS OF NUMERICAL CALCULATIONS

To illustrate the properties of Bragg reflections from magnetically ordered crystals, we present the results of the calculation of the diffraction of resonant 14.4 keV  $\gamma$  radiation of the isotope  $Fe^{57}$  by a thick perfect ferromagnetic iron crystal at room temperature.

The reflection curves of radiation with polarizations that coincide with the eigenpolarizations (polarization vectors  $n_1$  and  $n_2$ ) are shown in Fig. 2. The calculations were performed for the reflection (110) ( $2\theta_b = 24.5^\circ$ ) from an iron single crystal enriched with  $Fe^{57}$  up to 80%, the  $\gamma$ -quantum energy coincides with the energy of the energy of the  $3/2 - 1/2$  transition, and the angle  $\Phi$  is equal to zero. It is assumed here and below that the magnetic field  $H$  lies in the scattering plane and  $\Phi$  is the angle between  $H$  and the scattering plane.

The qualitative difference between the two curves of Fig. 2 is due to the polarization dependence of the nuclear resonant scattering. Curve 1 corresponds to polarization of the scattering beam, which is very close to the polarization  $n_1$  that ensures maximum amplitude of the nuclear scattering through the  $3/2 - 1/2$  transition for a  $\gamma$  quantum propagating in the  $k_1$  direction, and has the form typical of purely nuclear resonant scattering. The polarization of the scattered radiation is close here to the polarization  $n_1'$  that ensures maximum amplitude of the nuclear scattering for a  $\gamma$  quantum propagating in the direction  $k_2$ . Curve 2 corresponds to polarization of the primary beam very close to the polarization  $n_2'$  ( $n_2'$  stands for a vector orthogonal to  $n_2$ ), for which the amplitude of the nuclear scattering in the  $3/2 - 1/2$  transition vanishes and takes a form typical of Rayleigh scattering. In this case the polarization of the scattered radiation is close to  $n_2'$ .

The variations of the polarization along the reflection curves 1 and 2 are shown in Fig. 3. The dashed line pertains to polarization of the incident wave, and the solid lines to the scattered wave. The polarization in Fig. 3 is described by two parameters  $\alpha$  and  $\varphi$ , where  $\tan\alpha$  is the ratio of the axes of the polarization ellipse and  $\varphi$  is the angle between the major axis of the polarization ellipse and the scattering plane. As seen from the figure, the polarizations of the scattered (re-

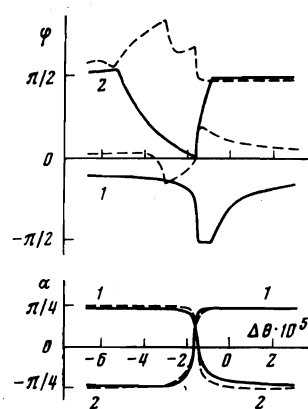


FIG. 3. Angular dependence of the parameters  $\alpha$  and  $\varphi$ , which describe the polarization of the eigenwaves (the solid and dashed curves pertain to the scattered and transmitted waves, respectively). The values of the parameters are the same as in Fig. 2.

flected) waves along the reflection curves 1 and 2 are elliptic, are not orthogonal to each other, undergo rapid changes in a small section of the reflection curve, and tend in the limit as  $|\Delta\theta| \rightarrow \infty$  to the eigenpolarizations for direct transmission (close to  $n_t$  and  $n_t^\perp$ ).

Calculations show that the dimensions of the region in which a strong change takes place in the natural polarizations depend on the ratio of the nuclear and Rayleigh scattering amplitudes. If the nuclear amplitude exceeds the Rayleigh amplitudes, then the region of variation of the polarization turns out to be much smaller than the region of diffraction reflection. In the characteristic that are integral with respect to the angles, the change of the eigenpolarizations can be neglected and it can be assumed that in the entire reflection region they coincide with  $n_t$  and  $n_t^\perp$  ( $n_t$  and  $n_t^\perp$ ). The shapes of the reflection curves corresponding to different polarizations turn out to have significantly different dependences on the  $\gamma$ -quantum energy. The form of curve 1 depends on the  $\gamma$ -quantum energy and reveals the interference of the nuclear and Rayleigh scattering. The reflection coefficient for the second eigenpolarization has a characteristic Rayleigh shape and remains practically unchanged when the energy varies near resonance. By virtue of this fact, at  $\gamma$ -quantum energies corresponding to constructive interference of the nuclear and Rayleigh scattering, the larger area is the one under curve 1, and quanta with polarization  $n_t$  will predominate in the scattered radiation (Fig. 4a). However, if the energy of the incident radiation is such that the nuclear and Rayleigh scatterings cancel each other in maximum fashion (Fig. 4b), then the angular dimensions of the region of scattering of  $\gamma$  quanta with polarization  $n_t^\perp$  may turn out to be larger. The curves shown in Figs. 4a and 4b were obtained at  $E = E_{3/2-1/2} + 2\Gamma$  and  $E = E_{3/2-1/2} - 4\Gamma$ , respectively.

The calculation results presented above pertain to a  $\gamma$ -ray energy close to resonance, and yield scattering characteristics, particularly polarizations, which are very close to the values corresponding to scattering via the single transition  $3/2 - 1/2$ . At a considerable distance from resonance, and even near the resonant Zeeman transition, which corresponds to a small amplitude of the nuclear scattering, several Zeeman transitions become significant and the scattering characteristics, including the polarization characteristics, are no longer determined by a single transition (see below).

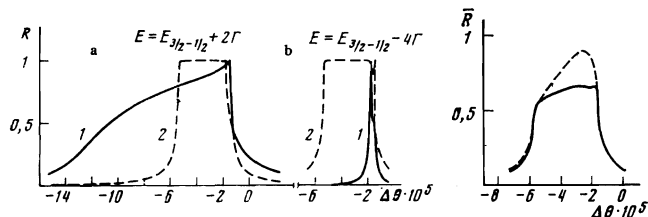


FIG. 4

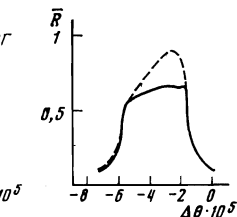


FIG. 5

FIG. 4. Reflection coefficient of the eigenwaves in constructive (a) and destructive (b) interference of nuclear and Rayleigh scattering (curve 1 is shown solid and curve 2 dashed). Curves (a) were obtained at  $E = E_{3/2-1/2} + 2\Gamma$ , and curves (b) at  $E = E_{3/2-1/2} - 4\Gamma$ . The remaining parameters are the same as in Fig. 2.

FIG. 5. Influence of non-orthogonality of the eigenwaves on the reflection coefficient of unpolarized radiation (solid curve). The dashed curve shows the arithmetic mean of the reflection curves for the eigenpolarizations.  $E = E_{1/2-1/2}$ ,  $\Phi = 20^\circ$ . The remaining parameters are the same as in Fig. 2.

Owing to the non-orthogonality of the polarizations for curves 1 and 2 (Fig. 2), the reflection coefficient for the unpolarized radiation, in accordance with formula (24), differs from the arithmetic mean of curves 1 and 2. For the curve shown in Fig. 2, this non-orthogonality is small, and the difference between the reflection coefficient and the arithmetic mean of the two curves is not significant. In the general case, however, the effect connected with the non-orthogonality can be quite large. This is illustrated in Fig. 5, on which the arithmetic mean of the two reflection curves is shown by the dashed line, and the reflection coefficient, calculated from formula (24), is given by the solid line. The curves were obtained for  $\Phi$  equal to  $20^\circ$  and for a  $\gamma$ -ray energy coinciding with the energy of the  $1/2 - 1/2$  transition.

The energy dependence of the integrated characteristics of the scattering is illustrated by Figs. 6 and 7. The integrated reflection coefficient  $R$ , the degree of polarization  $P$ , and the parameters  $\alpha$  and  $\varphi$  that describe the polarization represented in the scattered radiation are given for two magnetic-field directions ( $\Phi = 0$  and  $\Phi = 60^\circ$ ) at an incident-beam energy width coinciding with the natural width of the Mössbauer line. In the lower diagram, the energy dependences of  $\alpha$  and  $\varphi$  are shown solid and dashed, respectively.

The integrated-reflection curves demonstrate clearly the influence of the direction of the magnetic field at the nuclei on the intensity of the reflected radiation. The case  $\Phi = 0$  is characterized by the fact that nuclear scattering sufficiently large for transition with  $M = \pm 1$  turns out to be greatly attenuated for transitions with  $M = 0$ . This is manifest in the form of the energy dependence of the integral reflection coefficient. In the region of transitions with  $M = 0$ , the scattering exhibits minima, whereas near transitions with  $M = \pm 1$  the reflection coefficient has a clearly pronounced dispersion form, reaching a minimum on one side of the exact resonant value of the energy and a maximum on the other. At a magnetic-field orientation corresponding to

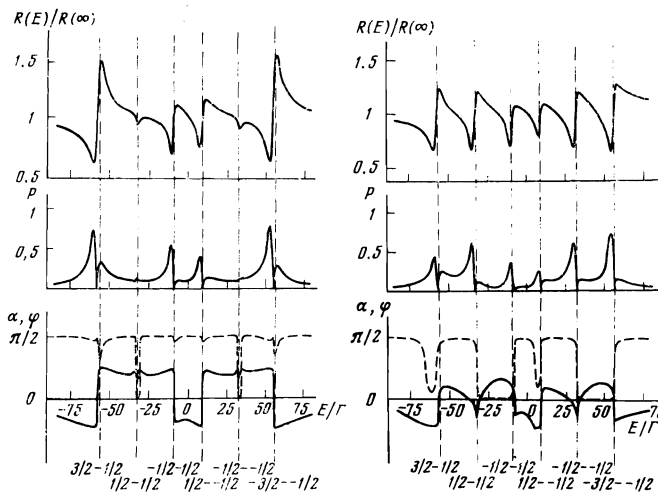


FIG. 6

FIG. 7

FIG. 6. Energy dependences of the integrated reflection coefficient  $R$ , of the degree of polarization of the scattered radiation  $P$ , of the parameters  $\alpha$  and  $\varphi$  for Bragg reflection (110) of an unpolarized  $\gamma$ -ray beam from an iron single crystal. The vertical dashed lines show the positions of the nuclear resonances.  $\eta = 80\%$ ,  $\Phi = 0^\circ$ , the energy width of the incident beam coincides with the width of the Mössbauer line.

FIG. 7. The same as in Fig. 6. Angle  $\Phi = 60^\circ$ .

$\Phi = 60^\circ$ , the amplitudes of the nuclear scattering via the transitions with  $M = 0$  and  $M = \pm 1$  are comparable in magnitude, and the energy dependence of the reflection coefficient for all the lines in the spectrum has a dispersion form.

The degree of polarization of the scattered radiation, being a function of the  $\gamma$ -quantum energy, is sufficiently high near the resonances for which the amplitude of the nuclear scattering is not small in comparison with the Rayleigh scattering, and has two maxima near these resonances. The maximum to the left of the resonance corresponds to the value of  $E$  at which the nuclear and Rayleigh scatterings cancel each other in maximum fashion. The integrated intensity has a dip in this case, and the vector of the partial polarization is close to  $n_{\perp}^{\perp}$ . The second maximum of the degree of polarization, located to the right of the resonance, is realized at an energy value corresponding to constructive interference between the nuclear and electron scatterings. The corresponding integrated reflection coefficient is maximal in this case, and it is quanta with polarization close to  $n_{\parallel}^{\parallel}$  that are mainly represented in the scattering.

The curves show that by changing the direction of the magnetic field in the crystal, or by tuning to different resonance, it is possible to change appreciably the polarization of the scattered radiation. Thus, coherent scattering of  $\gamma$  radiation by a ferromagnetic crystal yields highly-polarized  $\gamma$ -ray beams of practically any polarization (although the incident radiation not polarized).

## 7. CONCLUDING REMARKS

The results of the preceding sections show that Mössbauer scattering by magnetically-ordered crystals, and primarily its polarization characteristics, have many qualitative features that do not appear in Mössbauer scattering by paramagnetic crystals. These features become most clearly pronounced in the differential cross section for the scattering of polarized quanta (and in the detection of the polarization of the scattered radiation). This is clearly demonstrated by the fact that the reflection curve has a quantitatively different form than in the case of the unsplit line (see Fig. 1), and also by the constancy of the polarizations of the eigensolutions along the reflection curve. Since the characteristics measured in the experiment are usually integrated (with respect to the angle or energy), we shall dwell here on the manifestation of these features in the integral quantities.

For unpolarized primary radiation, the character of the polarization of the scattered radiation is determined directly by the magnetic structure of the crystal, i.e., it depends on the orientation of the magnetic moments of the atoms and on their positions in the unit cell, and the degree of polarization of the scattered radiation (which depends in the general case on the  $\gamma$ -ray energy) can become comparable with unity (see Fig. 7). Therefore, in addition to the above-noted possibility of extracting information on the magnetic structure of the

crystal from an analysis of the polarization of the scattered radiation, Mössbauer scattering affords the possibility of obtaining polarized  $\gamma$ -ray beams. By varying the orientation of the magnetic moments in the crystal (for example, by applying an external field), it is easy to change the polarization of the scattered radiation. In the case of a ferromagnetic crystal, it is possible to obtain in this manner practically any polarization (from linear to circular) of the scattered radiation.

The specific features of scattering from magnetically ordered crystals is manifest also when no polarization measurements are made (the initial beam is not polarized, and the polarization of the scattered radiation is not detected). In this case, for example, the energy dependence of the integrated reflection turns out to be different than in the case of the unsplit line. The reason for this is the non-orthogonality of the polarizations of the eigensolutions and the related energy dependence of the interference terms in expressions (13) and (19), from which the integrated reflection coefficient is determined.

- <sup>1</sup>A. M. Afanas'ev and Yu. Kagan, Zh. Eksp. Teor. Fiz. 48, 327 (1965) [Sov. Phys.-JETP 21, 215 (1965)].
- <sup>2</sup>G. S. Zhdanov and R. N. Kuz'min, Acta Cryst., B24, 10 (1968).
- <sup>3</sup>V. A. Belyakov and Yu. M. Aivazyan, ZhETF Pis. Red. 7, 477 (1968) [JETP Lett. 7, 368 (1968)]. Phys. Rev. B1, 1903 (1970).
- <sup>4</sup>V. K. Voïtovetskiĭ, I. L. Korsunskiĭ, A. I. Novikov, and Yu. F. Pazhin, ZhETF Pis. Red. 8, 611 (1968) [JETP Lett. 8, 376 (1968)].
- <sup>5</sup>G. V. Smirnov, V. V. Sklyarevskii, R. A. Voskanyan, and A. I. Artem'ev, ZhETF Pis. Red. 9, 123 (1969) [JETP Lett. 9, 70 (1969)].
- <sup>6</sup>D. A. O'Connor and E. R. Spiecer, Phys. Lett., 29A, 136 (1969).
- <sup>7</sup>R. M. Mirzababaev, G. V. Smirnov, V. V. Sklyarevskii, A. N. Artem'ev, A. N. Izrailenko, and A. V. Bobkov, Phys. Lett., 37A, 441 (1971).
- <sup>8</sup>R. L. Mössbauer and U. Biebl, Zs. Phys., 244, 456 (1971).
- <sup>9</sup>V. A. Belyakov, Fiz. Tverd. Tela 13, 2170 (1971) [Sov. Phys.-Solid State 13, 1824 (1972)].
- <sup>10</sup>A. M. Afanas'ev and Yu. Kagan, Zh. Eksp. Teor. Fiz. 64, 1958 (1973) [Sov. Phys.-JETP 37, 987 (1973)].
- <sup>11</sup>Yu. M. Aivazyan and V. A. Belyakov, Zh. Eksp. Teor. Fiz. 56, 346 (1969) [Sov. Phys.-JETP 29, 191 (1969)].
- <sup>12</sup>A. M. Afanas'ev and I. P. Perstnev, Zh. Eksp. Teor. Fiz. 65, 1271 (1973) [Sov. Phys.-JETP 38, 630 (1974)].
- <sup>13</sup>B. W. Batterman and H. Cole, Rev. Mod. Phys., 38, 681 (1964).
- <sup>14</sup>G. T. Trammell, Phys. Rev., 126, 1045 (1962).
- <sup>15</sup>Yu. M. Aivazyan and V. A. Belyakov, Fiz. Tverd. Tela 13, 968 (1971) [Sov. Phys.-Solid State 13, 808 (1971)].

Translated by J. G. Adashko

69